

Radiation Chemistry in Solvent Extraction: FY 2010 Research

Bruce Mincher
Leigh R. Martin
Stephen P. Mezyk

September 2010



The INL is a U.S. Department of Energy National Laboratory
operated by Battelle Energy Alliance

Radiation Chemistry in Solvent Extraction: FY 2010 Research

**Bruce Mincher
Leigh R. Martin
Stephen P. Mezyk**

September 2010

**Idaho National Laboratory
Fuel Cycle Research & Development
Idaho Falls, Idaho 83415**

<http://www.inl.gov>

**Prepared for the
U.S. Department of Energy
Office of Nuclear Energy
Under DOE Idaho Operations Office
Contract DE-AC07-05ID14517**

DISCLAIMER

This information was prepared as an account of work sponsored by an agency of the U.S. Government. Neither the U.S. Government nor any agency thereof, nor any of their employees, makes any warranty, expressed or implied, or assumes any legal liability or responsibility for the accuracy, completeness, or usefulness, of any information, apparatus, product, or process disclosed, or represents that its use would not infringe privately owned rights. References herein to any specific commercial product, process, or service by trade name, trade mark, manufacturer, or otherwise, does not necessarily constitute or imply its endorsement, recommendation, or favoring by the U.S. Government or any agency thereof. The views and opinions of authors expressed herein do not necessarily state or reflect those of the U.S. Government or any agency thereof.

ABSTRACT

This report summarizes work accomplished under the Fuel Cycle Research and Development (FCR&D) program in the area of radiation chemistry during FY 2010. The tasks assigned during FY 2010 included:

- Development of techniques to measure free radical reaction kinetics in the organic phase.
- Initiation of an alpha-radiolysis program
- Initiation of an effort to understand dose rate effects in radiation chemistry
- Continued work to characterize TALSPEAK radiation chemistry

Progress made on each of these tasks is reported here. Briefly, a method was developed and used to measure the kinetics of the reactions of the $\bullet\text{NO}_3$ radical with solvent extraction ligands in organic solution, and the method to measure $\bullet\text{OH}$ radical reactions under the same conditions has been designed. Rate constants for the CMPO and DMDOHEMA reaction with $\bullet\text{NO}_3$ radical in organic solution are reported. Alpha-radiolysis was initiated on samples of DMDOHEMA in alkane solution using He ion beam irradiation and ^{211}At isotope irradiation. The samples are currently being analyzed for comparison to DMDOHEMA γ -irradiations using a custom-developed mass spectrometric method. Results are also reported for the radiolytic generation of nitrous acid, in γ -irradiated nitric acid. It is shown that the yield of nitrous acid is unaffected by an order-of-magnitude change in dose rate. Finally, recent results for TALSPEAK radiolysis are reported, summarizing the effects on solvent extraction efficiency due to HDEHP irradiation, and the stable products of lactic acid and DTPA irradiation.

In addition, results representing increased scope are presented for the radiation chemistry program. These include an investigation of the effect of metal complexation on radical reaction kinetics using DTPA as an example, and the production of a manuscript reporting the mechanism of Cs-7SB radiolysis. The Cs-7SB work takes advantage of recent results from a current LDRD program to understand the fundamental chemistry of nitration under radiolysis conditions. Finally, work toward understanding the chemistry of irradiated formic acid is presented. This is important because all organic compounds eventually produce formic acid under long-term irradiation.

CONTENTS

ABSTRACT.....	iii
ACRONYMS.....	vii
1. INTRODUCTION.....	1
2. RESULTS AND DISCUSSION.....	1
2.1 Kinetics in the organic phase	1
2.1.1 •NO ₃ radical kinetics in the organic phase.....	1
2.1.2 •OH radical kinetics in the organic phase	3
2.2 Alpha radiolysis	4
2.3 Dose rate effects.....	6
2.4 TALSPEAK Radiation Chemistry	7
2.4.1 Effect of Radiolysis on pH.....	7
2.4.2 Effect of Radiolysis on HDEHP and the Extraction of Europium.....	7
2.4.3 Stable Product Identification.....	10
2.5 Additions to work scope	12
2.5.1 Metal Complexed Ligands.....	12
2.5.2 Cs-7SB radiation chemistry	14
2.5.3 Formic Acid/Oxalic Acid Radiolysis.....	16
3. CONCLUSIONS AND FUTURE WORK.....	17
4. LITERATURE CITED.....	18

FIGURES

Figure 1. The UV/Vis absorbance spectrum of the •NO ₃ radical in <i>t</i> -butanol solution. The spectrum is shifted to about 10 nm lower in wavelength in the organic solution.....	3
Figure 2. TM-DESI-MS mass spectrum of irradiated DMDOHEMA.....	4
Figure 3. Dissolution of the astatine-containing bismuth target to separate ²¹¹ At from target material using nitric acid. The target is shown prior to dissolution on the plate to the left, with the aluminum target backing shown on the right.	5
Figure 4. The yield of HNO ₂ at dose rates of 10 kGy h ⁻¹ (circles) and 1 kGy h ⁻¹ (diamonds) for 4 M (filled symbols) and 2 M (open symbols) γ-irradiated HNO ₃	6
Figure 5. Variation of pH in irradiated lactic acid solutions as a function of absorbed dose. (■) 0.001M lactic acid, (●) 0.01M lactic acid and (▲) 1.0 M lactic acid.	7
Figure 6. Distribution ratios for europium and americium versus absorbed γ dose for irradiated 0.17 M, 99.9% pure HDEHP in dodecane. No aqueous phase was present during irradiation. The extraction was performed from 1.0 M lactic acid, 50 mM DTPA at pH 3.8. Error bars shown are standard deviations of triplicate measurements.....	8
Figure 9. HPLC diode array chromatogram for 0.001 M sodium lactate at pH 3.8 irradiated to 35 kGy.	11

Figure 10. HPLC diode array chromatogram for 1:10 dilution DTPA irradiated to 200 kGy.....	11
Figure 11. Occurrence of DTPA protonation species versus solution pH. Six species occur, from fully protonated to fully deprotonated.	13
Figure 12 The linear transform plot (left) gives the bimolecular rate constant for the •OH radical reaction with DTPA. The decrease in SCN ₂ absorbance with increasing DTPA concentration is shown on right.	13

TABLES

Table 1. Rate constants ($M^{-1} s^{-1}$) for the reaction of •NO ₃ radical in organic and aqueous solution.....	2
Table 2. Summary of speciation and measured •OH radical reaction rate constants for DTPA at different pHs.	14
Table 3. Summary of reaction rate constants for hydroxyl radical, hydrogen atom, and nitrate radical with Cs-7SB and analogues. Reaction rates for the •NO ₂ radical were below detection limit of $\sim 10^6 M^{-1} s^{-1}$	16

ACRONYMS

CSULB	California State University- Long Beach
CMPO	octylphenyldiisobutylcarbamoylmethylphosphine oxide
Cs-7SB	1-(2,2,3,3,-tetrafluoropropoxy)-3-(4-sec-butylphenoxy)-2-propanol
DMDOHEMA	dimethyl dioctyl hexylethoxymalonamide
DTPA	ethylenediaminepentaacetic acid
FCR&D	Fuel Cycle Research and Development
HDEHP	diethylhexylphosphoric acid
H ₂ MEHP	monoethylhexylphosphoric acid
HPLC	High Pressure Liquid Chromatography
INL	Idaho National Laboratory
LDRD	Lab Directed Research and Development program
LET	linear energy transfer
MF2-BTBP	4- <i>t</i> -butyl-6,6'-bis(5,5,8,8,-tetramethyl-5,6,7,8-tetrahydro-benzo[1,2,4]triazin-3-yl)
-bypyridine	
MOA	methyloctylamine
NEUP	Nuclear Energy University Programs
NDRL	Notre Dame Radiation Laboratory
PUREX	plutonium uranium refining by extraction process
TALSPEAK	Trivalent Actinide Lanthanide Separation by Phosphorous reagent Extraction from Aqueous Komplexes
TBANO ₃	tetrabutylammonium nitrate
TBP	tributylphosphate
TRUEX	transuranic extraction process
TM-DESI-MS	transmission mode desorption electrospray ionization mass spectrometry
UCI	University of California, Irvine
UREX	uranium extraction process
UV/Vis	ultraviolet/visible spectroscopy

SEPARATIONS AND WASTE FORMS/RADIATION CHEMISTRY PROGRAM

1. INTRODUCTION

During aqueous solvent extraction separations for fuel cycle applications the organic solvent is irradiated with both high linear energy transfer (LET) alpha and low LET beta/gamma radiation. The deposition of this energy into the system may result in adverse effects including degradation of ligands and loss of solvent extraction efficiency, production of radiolysis products that complex metals to decrease separation factors, and possible changes in physical characteristics of the solvent due to precipitates or polymers. For application in a nuclear solvent extraction process, components of the solvent formulation must have adequate radiolytic stability to ensure solvent recycle potential. The ligand decomposition yield should be sufficiently low, and the nature of the decomposition products sufficiently benign, that significant process efficiency is not lost with time and absorbed radiation dose. Therefore, a major effort in the separations campaign has been invested in understanding radiation chemistry in biphasic, acidic systems containing the ligands of most importance to the proposed future fuel cycle.

When a radiation event occurs in solution, direct interaction of the incident particle with a solution constituent can only happen in proportion to the abundance of that component. Therefore, the diluent is the most likely solution component to be affected. Diluent radiolysis produces ionic and radical species that may diffuse through the solution to react with other diluent molecules, or the ligands designed to complex metal ions for separations. Radical reactions are especially important, and knowledge of the rate constants for these reactions and the reaction products allows reaction mechanisms to be elucidated. Therefore, a successful radiation chemistry program will consist of a strong kinetics component, relying on pulse radiolysis, and a strong analytical chemistry component, relying on mass spectrometric, liquid chromatographic and other appropriate methods. These techniques have been employed in the work reported here.

This report summarizes those efforts for FY 2010. Only the highlights are presented here, for further information the cited journal publications need be consulted. The results of four major assigned tasks and three additional tasks representing increased scope are presented. These tasks include the development of methods to measure radical kinetics in the organic phase, initiation of alpha radiolysis studies, initiation of dose rate dependence studies and recent findings in TALSPEAK radiolysis. Increased scope tasks include initiation of a program to evaluate the effects of metal complexation on ligand radiolysis, preparation of a manuscript elucidating the radiolysis mechanism of Cs-7SB, and an effort to understand formic acid chemistry.

2. RESULTS AND DISCUSSION

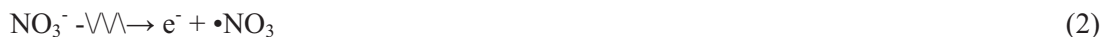
2.1 Kinetics in the organic phase

Conventional pulse radiolysis is conducted in the aqueous phase. However, in the irradiated solvent extraction system, an organic phase is in contact with the aqueous phase, and neutral radicals may also undergo reactions in that organic phase. Radicals such as $\bullet\text{OH}$ and $\bullet\text{NO}_3$ that are produced in the aqueous phase may diffuse across the phase boundary, or they may be produced *in-situ* from extracted acid and water. To model these reactions it is necessary to measure the kinetic constants for the organic phase.

2.1.1 $\bullet\text{NO}_3$ radical kinetics in the organic phase

Previously under this program the technique was developed for the generation and measurement of the $\bullet\text{NO}_3$ radical in the aqueous phase (Mincher et al 2008). This was achieved using pulse-irradiated, N_2O -

sparged 6 M HNO₃. Under these conditions the production of the •NO₃ radical is maximized by direct radiolysis of nitrate and nitric acid shown in eqs. 1 and 2:

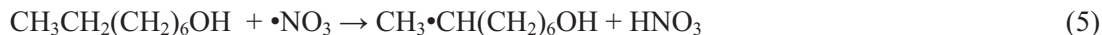


Additional •NO₃ radical is produced by the reaction of undissociated HNO₃ with the •OH radical (eq. 3), and •OH radical production is maximized by reaction of solvated electrons with the N₂O (eq. 4):



The •NO₃ radical produced in this way is then monitored by following its absorbance at 640 nm versus time, allowing for the measurement of the required rate constants.

However, an organic-soluble source of nitrate was necessary to generate •NO₃ radical in the organic phase. Tetrabutyl ammonium nitrate (TBANO₃) was found to have a solubility of ~ 1.4 M in both *n*-octanol and *t*-butanol. When an *n*-octanol solution of TBANO₃ was pulse irradiated, no •NO₃ radical was measureable. This may be because of a very fast reaction between the •NO₃ radical and the alcohol itself, which would react with alkane CH₂ groups by H-atom abstraction:



Pulse radiolysis of TBANO₃ in *t*-butanol, which lacks CH₂ groups, was more successful. The absorbance spectrum of the •NO₃ radical in this organic solution is shown in Fig 1. The spectrum is similar to that which was previously reported under this program in aqueous solution (Mincher et al 2008), although slightly blue shifted. The absorbance maximum at 630 nm was used to measure the kinetic constants for the reaction of •NO₃ radical with CMPO and DMDOHEMA in *t*-butanol solution. The rate constant for the reaction of octanol in *t*-butanol solution was also determined. These data are given in Table 1, along with the previously determined rate constants for these reactions in aqueous solution.

Table 1. Rate constants (M⁻¹ s⁻¹) for the reaction of •NO₃ radical in organic and aqueous solution.

Analyte	<i>t</i> -BuOH	aqueous
CMPO	(9.33±0.59) x 10 ⁷	(1.28±0.13) x 10 ⁸
DMDOHEMA	(4.27±0.46) x 10 ⁸	(2.22±0.10) x 10 ⁸
octanol	(4.33±0.43) x 10 ⁸	5.8 x 10 ⁶

Due to the limited solubility of CMPO and DMDOHEMA in aqueous solution, 20% acetone was used as a cosolvent, resulting in a final nitric acid concentration of 4.8 M for those measurements. There is no obvious trend between solvents with the rate constant being lower in the organic phase for CMPO, and higher for DMDOHEMA and octanol. The rate constant for octanol is important since it represents the rate for •NO₃ reaction with the diluent. A fast rate of reaction with the diluent indicates that less radical will be available to react with the lower concentration of ligand. For example, note that the rate constants for DMDOHEMA and octanol are nearly identical in the *t*-butanol solution. Since in the proposed solvent extraction process DMDOHEMA is used at a concentration of 0.65 M and octanol at 6.3 M, only approximately 10% of •NO₃ radical yield in the organic phase would be available to react with the ligand under these conditions. This rate constant also explains why no •NO₃ radical was detected in irradiated octanol solutions of TBANO₃, since the high concentration of octanol would quickly scavenge and produce radical.

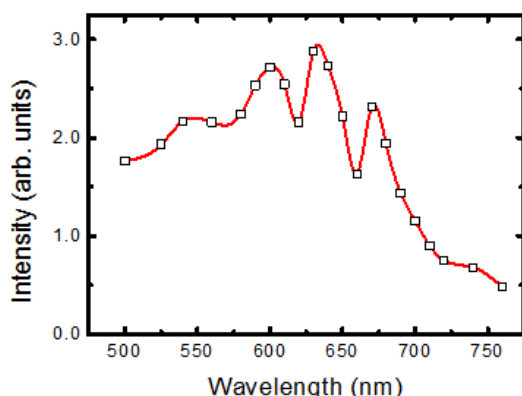


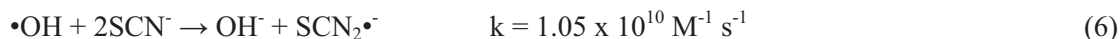
Figure 1. The UV/Vis absorbance spectrum of the $\bullet\text{NO}_3$ radical in *t*-butanol solution. The spectrum is shifted to about 10 nm lower in wavelength in the organic solution.

In future experiments we will examine higher C-chain length alcohols, using branch chain alcohol addition to *t*-butanol solution. Branch chain species minimize scavenging of $\bullet\text{NO}_3$ by reactions such as that shown in eq. 5. This will allow us to estimate rates of reaction of ligands with $\bullet\text{NO}_3$ radical in the alkane solvents used for CMPO solvent extraction. However, it can be tentatively concluded that diluents containing abundant $-\text{CH}_2-$ groups will scavenge $\bullet\text{NO}_3$ radical resulting in protection of the ligands. However, it should be kept in mind that nitrated alkanes have been implicated in solvent degradation for the PUREX process (Tahraoui and Morris 1995).

2.1.2 $\bullet\text{OH}$ radical kinetics in the organic phase

Similarly to the $\bullet\text{NO}_3$ radical discussion above, $\bullet\text{OH}$ radical kinetics have only been measured in the aqueous phase. In general, their reaction rates are faster than those of $\bullet\text{NO}_3$ radical.

New techniques for the generation of $\bullet\text{OH}$ radical in the organic phase are currently under development. Although salts such as KOH have reasonable solubility in *t*-butanol, the reaction of OH^- with the solvated electron is not expected to provide $\bullet\text{OH}$. However, a wet organic solvent might be used in conjunction with N_2O sparging to yield $\bullet\text{OH}$ as shown in eq. 4 above. A further complicating factor is that the $\bullet\text{OH}$ radical has no useful UV/Vis absorbance and it must be detected indirectly. This is usually done using KSCN according to eq. 6:



The produced $\text{SCN}_2\bullet^-$ radical absorbs strongly at 475 nm and is used to indirectly observe the $\bullet\text{OH}$ radical. We propose to create the $\bullet\text{OH}$ radical in *t*-butanol solution containing small amounts of water, which we anticipate will solvate KSCN. This will be attempted at the next available NDRL beam time opportunity.

Alternately, $\bullet\text{OH}$ may be created in the organic phase using laser flash photolysis (Mitroka et al 2010). In that work, the photo-labile $\bullet\text{OH}$ radical precursor hydroxypyridine-2-thione was photolyzed at 355 nm to generate $\bullet\text{OH}$ radical. UV detection of the $\bullet\text{OH}$ radical addition product of the reaction with trans-stilbene at 392 nm was used to monitor $\bullet\text{OH}$ reaction chemistry, in analogy with the thiocyanate competition kinetics discussed above. Laser flash photolysis equipment is available at the US DOE Notre Dame Radiation Laboratory, South Bend, IN (NDRL) lab where the pulse radiolysis experiments are conducted, and this technique will serve as a back-up plan if wet solvent pulse radiolysis proves untenable.

2.2 Alpha radiolysis

The linear energy transfer (LET) of an α particle is significantly greater than that of β, γ radiation. Massive, highly charged α -particles have short ranges and deposit 156 eV nm^{-1} at an energy of 5 MeV (Pastina and Laverne 1999) in water. They therefore deposit energy in closely-spaced overlapping spurs, resulting in high localized concentrations of reactive species, many of which undergo recombination before they can diffuse into the bulk solution. The result is higher yields of molecular species and lower yields of radicals. Therefore, differences in the effects of irradiation between high and low LET sources might be expected. Most radiation chemistry studies have been performed using γ -sources for ease of contamination control and post-irradiation analytical chemistry. However, solvents used for the solvent extraction of metals from dissolved fuel will also be exposed to significant α -doses. It is therefore desirable to understand the effects of high LET radiation, and a α -radiolysis program was initiated in FY 2010.

Recently, a number of reports have found that α radiolysis results in less radiolytic damage to solvent extraction systems than γ irradiation (Magnussen et al 2009, Sugo et al 2009, Camès 2010). These are in contrast to a report for the TRUEX solvent which found greater degradation due to α irradiation (Buchholz et al 1996). However, no detailed studies that include product identification have been done on the α -radiolysis of solvent extraction solvents. Here, a program was initiated to better understand α -radiolysis in collaboration with NEUP partners at California State University-Long Beach (CSULB) and University of California-Irvine (UCI) (Mezyk et al 2010). Three techniques are being compared in an effort to develop a standard method for these irradiations that is amenable to facile post-irradiation analytical chemistry. These techniques include He-ion beam irradiation, the use of boron neutron capture to create non-isotopic alpha particles at the UCI reactor, and isotopic α -sources, including ^{211}At .

The effort was initiated using the diamide ligand DMDOHEMA in alkane solution. Baseline data were collected using conventional γ -irradiation at the INL Gammacell 220. These samples were analyzed using a modified version of transmission mode desorption electrospray ionization mass spectrometry (TM-DESI-MS) in which the analyte solution was introduced via a target capillary (Groenewold et al 2010). In preliminary results using this technique, the observation of significant amounts of protonated methyloctylamine (MOA at m/z 144) indicates that radiolysis resulted in cleavage of the C-N bond of DMDOHEMA. The other product of the cleavage, presumably corresponding to the monoamide product, was not observed in the mass spectrum in these initial experiments. There was no evidence for cleavage of the hexylether moiety. These last observations are in contrast to the previous literature (Berthon et al 2001). The mass spectrum of irradiated DMDOHEMA is shown in Figure 2.

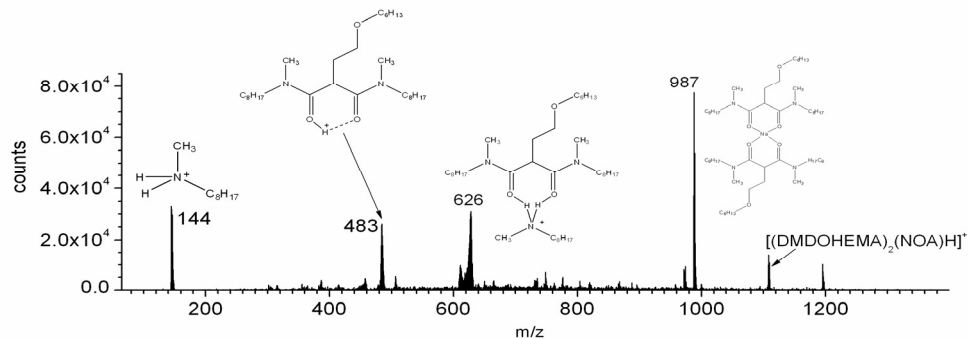


Figure 2. TM-DESI-MS mass spectrum of irradiated DMDOHEMA.

Similar samples were then irradiated using the He ion beam at the NDRL. Three samples were irradiated to an absorbed dose of 25 kGy in ocatnol, under aearated and degassed conditions. They are currently under analysis using the TM-DESI-MS technique for comparison.

Finally, another DMDOHEMA sample set was irradiated using ^{211}At at Chalmers University, Göteborg, Sweden. This technique was developed at Chalmers (Ekberg et al 2010). Astatine-211 is an ideal α -emitter for radiation chemistry studies because it decays with an average α energy of 6.8 MeV, and a half-life of 7.2 h to 32-year ^{207}Bi . The astatine is produced by irradiation of ^{209}Bi targets using 28 MeV α particles produced in a cyclotron. The reaction is shown in eq. 7.



The target was dissolved in nitric acid upon receipt (Fig. 3). The acidic solution containing dissolved bismuth and astatine was then adjusted to appropriate acidity, and the astatine was extracted into alkane solution using methods developed at Chalmers. Due to the high specific activity of the astatine parent the bismuth daughter is present at concentrations that are undetectable using both chemical and radiometric measurements. Being undetectable in the post-irradiation solution, the ease of post irradiation analytical chemistry is substantially increased as compared to conventional, long-lived, isotopic α -sources. This sample set is currently being shipped from Chalmers to INL for TM-DESI-MS analysis.

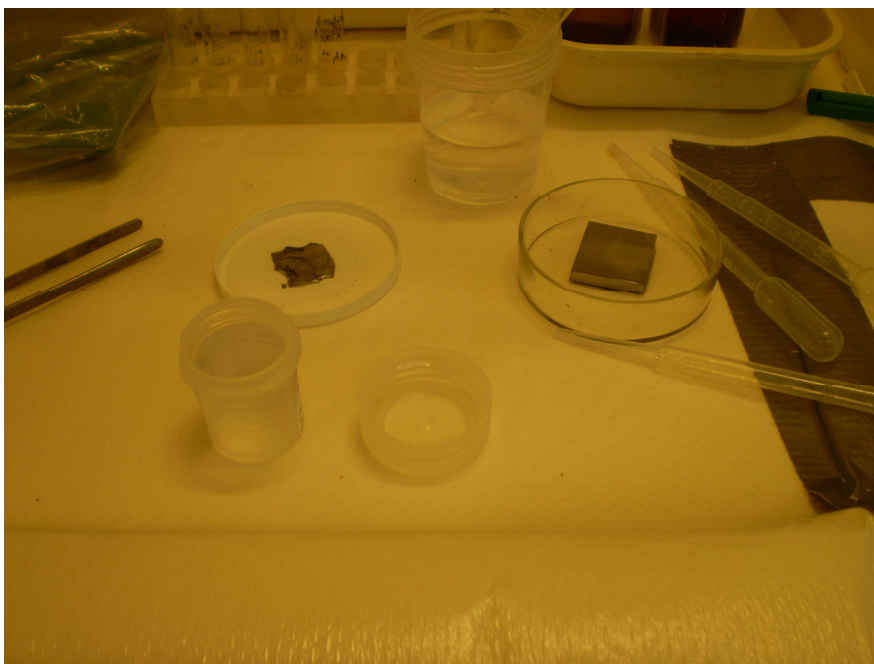


Figure 3. Dissolution of the astatine-containing bismuth target to separate ^{211}At from target material using nitric acid. The target is shown prior to dissolution on the plate to the left, with the aluminum target backing shown on the right.

2.3 Dose rate effects

Recently, it was reported that the use of varying γ -dose-rates for the irradiation of 0.01 M 4-*t*-butyl-6,6'-bis(5,5,8,8-tetramethyl-5,6,7,8-tetrahydro-benzo[1,2,4]triazin-3-yl)-bipyridine (MF2-BTBP) in cyclohexanone resulted in different effects on D_{Am} and D_{Eu} (Fermvik et al 2009). The solvent extraction efficiency of americium and europium was unchanged when the solutions were irradiated at 15 Gy h⁻¹, while distribution ratios decreased to about 60% of their initial value when the solutions were irradiated to the same absorbed dose at 1.2 kGy h⁻¹. However, these authors commented that the oxygen concentration was most likely higher in the solutions irradiated at the low dose-rate. Since irradiation of the pure organic phase in the absence of an aqueous phase results in a system dominated by reducing chemistry, the presence of higher concentrations of dissolved oxygen may explain the apparent dose rate effect through the scavenging of reducing radicals. However, it is important to understand if dose rate effects actually occur, because the dose rates to be encountered in the process are probably lower than most dose rates generated by γ -irradiators used under experimental conditions. To initiate these studies, the effect of dose rate on the radiolytic generation of nitrous acid was investigated.

It has been shown under previous work for this program that the radiolytic generation of HNO₂ in irradiated HNO₃ has consequences for both the nitration of ligands (Elias et al 2010, Swancutt et al in review) and metal oxidation states (Mincher 2010). Thus, the magnitude of its yield is important. The production of HNO₂ is shown in eqs. 8 and 9, and has both direct and indirect sources:



Here, the yield of HNO₂ in irradiated HNO₃ was measured using post-irradiation HPLC with UV detection. This was done for γ -dose rates of 10 kGy h⁻¹ and 1 kGy h⁻¹, using lead collimators to lower the dose rate in the INL ⁶⁰Co Gammacell. The results are shown in Fig. 1. It can be seen that the HNO₂ yield was unchanged over this order-of-magnitude dose rate range.

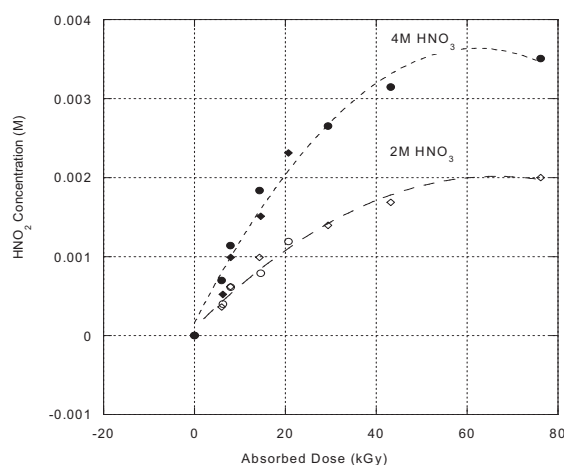


Figure 4. The yield of HNO₂ at dose rates of 10 kGy h⁻¹ (circles) and 1 kGy h⁻¹ (diamonds) for 4 M (filled symbols) and 2 M (open symbols) γ -irradiated HNO₃.

In general, an absence of dose rate effects is to be expected over the range of dose rates encountered using isotopic sources. However, continued work in this area is warranted. In future experiments the effect of changing dose rates on the radiation chemistry of the TRUEX solvent extraction process will be investigated using the Gammacell ^{60}Co source at INL.

2.4 TALSPEAK Radiation Chemistry

2.4.1 Effect of Radiolysis on pH

Any variation in the pH of the aqueous phase can adversely affect the separation efficiency of the TALSPEAK process (Nilsson and Nash 2007). Therefore, the radiolytic degradation of the lactic acid buffer could be problematic. To investigate this potential problem, solutions of lactic acid at three concentrations (1 mM, 10 mM and 1.0 M) were irradiated with the INL Gammacell ^{60}Co source to absorbed doses of 5, 10, 100 and 200 kGy. The pH of the lactate buffer solutions was measured before and after irradiation using a Ross combination pH electrode. In all cases the pH was seen to increase as a function of increasing dose with larger changes seen for smaller initial concentrations of lactic acid (Fig. 5). For the two lower lactic acid concentrations the pH appeared to stabilize at an absorbed dose of ~100 kGy. For the 1M initial lactate concentration, the pH of the solution was still increasing at an absorbed dose of 200 kGy, although the total pH change for this lactate concentration at the highest absorbed dose was only approximately 0.2 pH units. No discoloration was observed in the irradiated solutions at any absorbed dose, and no precipitates were formed suggesting that all degradation products are soluble in aqueous media.

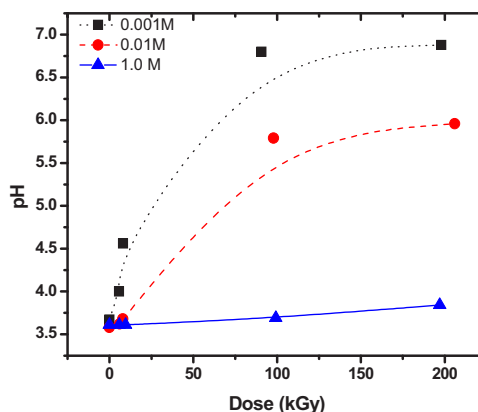


Figure 5. Variation of pH in irradiated lactic acid solutions as a function of absorbed dose. (■) 0.001M lactic acid, (●) 0.01M lactic acid and (▲) 1.0 M lactic acid.

2.4.2 Effect of Radiolysis on HDEHP and the Extraction of Europium

The change in distribution ratios for americium and europium as a function of absorbed dose to samples of 0.17 M HDEHP in dodecane, prepared from purified (99.9%) HDEHP, is shown in Figure 6. The irradiations were done in the absence of the aqueous phase. The distribution of europium is seen to slightly increase with increasing absorbed dose to the organic phase, whereas the distribution of americium is seen to decrease. Tachimori (1979) reported a similar effect for neodymium, when neat HDEHP was irradiated and then added to an alkane diluent to perform extractions. Increased extraction efficiency in the irradiated solvents can be attributed to the radiolytic production of mono-ethyl hexyl phosphoric acid (H_2MEHP) in the organic phase. As a slightly harder donor than HDEHP it would extract the lanthanides better than HDEHP alone.

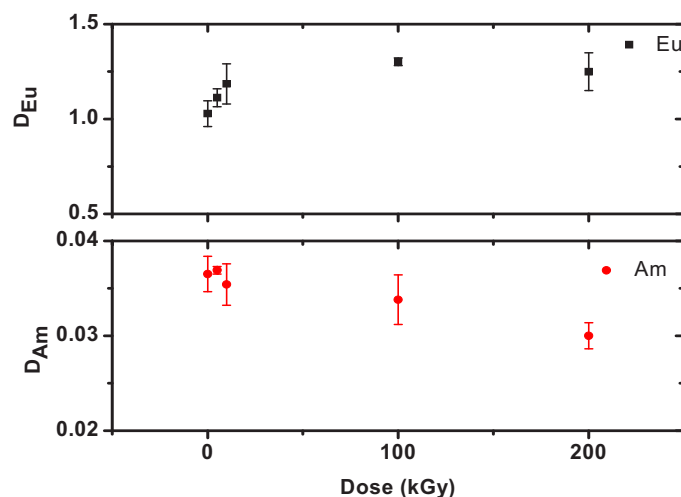


Figure 6. Distribution ratios for europium and americium versus absorbed γ dose for irradiated 0.17 M, 99.9% pure HDEHP in dodecane. No aqueous phase was present during irradiation. The extraction was performed from 1.0 M lactic acid, 50 mM DTPA at pH 3.8. Error bars shown are standard deviations of triplicate measurements.

It can also be seen by reference to Fig. 6 that americium distribution ratios decreased with absorbed dose under these conditions, possibly due to the hard donor H_2MEHP preference for the lanthanides. In previous work by Tachimori (1979) it was found that additions of H_2MEHP to HDEHP solutions produced similar effects to irradiation. However, it was also found that certain mole ratios of H_2MEHP to HDEHP increased americium extraction (Tachimori 1979b).

Irradiation experiments were also performed with the HDEHP samples in contact with a TALSPEAK aqueous phase, irradiated to similar doses (Fig. 7). In these experiments the distribution ratios for both americium and europium displayed an overall decrease with increasing absorbed dose. This suggests an absence of H_2MEHP in samples irradiated in the presence of an aqueous phase. This is also in agreement with Tachimori (1979), who found that when 0.5 M HDEHP in the alkane diluent was irradiated in the presence of 0.1 M HNO_3 , no H_2MEHP was produced. Instead, phosphoric acid was found, which complexed both neodymium and americium and suppressed their extraction. That author reported that when H_2MEHP was irradiated in dilute nitric acid, a high $-G$ -value for the loss of H_2MEHP of $6 \mu\text{mol J}^{-1}$ was measured, explaining both the absence of H_2MEHP and the presence of H_3PO_4 , which is the dealkylation product of H_2MEHP .

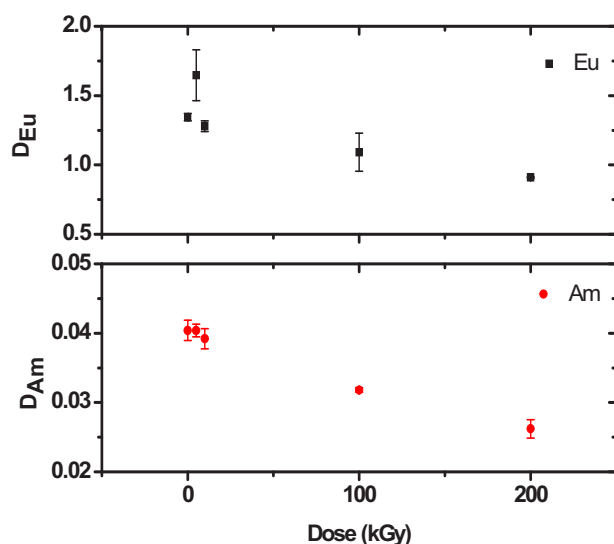


Figure 7. Distribution ratios for europium and americium versus absorbed dose to HDEHP/ lactic acid/ DTPA using 0.17M, 99.9 % pure HDEHP. Initial concentration of TALSPEAK extraction components was 1.0M lactic acid, 50mM DTPA at pH 3.8. Error bars shown are standard deviations of triplicate measurements.

This result is consistent with irradiation experiments performed here using a less pure (95%) HDEHP solution. The main impurity in the 95% HDEHP is expected to be H_2MEHP , and it can be seen in Fig. 8 that the initial distribution ratios for both americium and europium are higher than for pure HDEHP. For irradiated organic samples in the absence of the aqueous phase, there appears to be little change in the distribution ratios of both metals with increasing dose. There are at least two contributing factors to this result. The phosphoric acid degradation product of H_2MEHP partitions to the aqueous phase in post-irradiation extractions, and will act as a complexant for both metals. Secondly, the solvent extraction kinetics in TALSPEAK are slow, especially for europium and the heavier lanthanides. The partitioning of produced phosphoric acid is a complicating factor, and it is possible that these contacts were not at equilibrium, possibly explaining the higher errors associated with the distribution ratio measurements under these conditions. When these 95% pure HDEHP solutions were irradiated in contact with the aqueous phase, the results were similar to those for 99% pure HDEHP solution(Fig. 7), excepting the higher initial distribution ratios. The separation factor α_{AmEu} was not significantly impaired under the conditions studied.

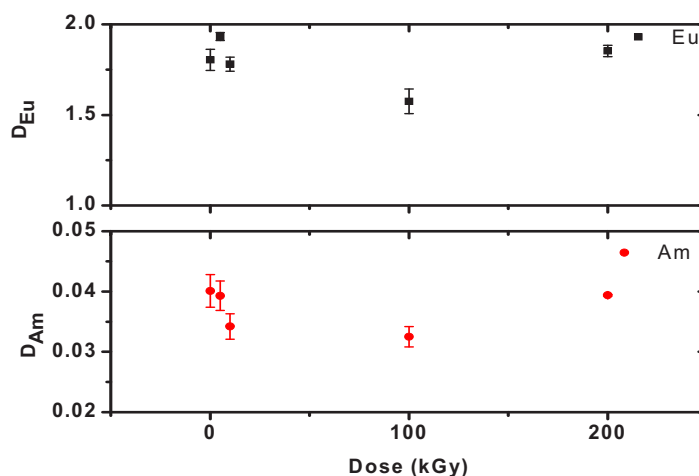


Figure 8. Distribution ratios for europium and americium versus absorbed dose to 0.17 M 95% pure HDEHP. TALSPEAK extraction performed from 1.0M lactic acid, 50mM DTPA at pH 3.8. Error bars shown are standard deviations of triplicate measurements.

2.4.3 Stable Product Identification

Following on from method development in FY 2009, progress has been made in identifying some of the degradation products of lactic acid and DTPA. Irradiated and non-irradiated samples of pH 1 lactic acid and pH 3.8 lactate buffer, at two concentrations (1 mM and 1.0 M) were analyzed by HPLC to identify significant degradation products. Of the new peaks observed, three have been identified as formic acid, oxalic acid and ethyl formate (Fig. 9). Formic acid is an important product since it is created by the oxidative degradation of all organic compounds, and its radiation chemistry is linked to the production of oxalic acid. A discussion of formic acid radiolysis is given in Section 1.5.3.

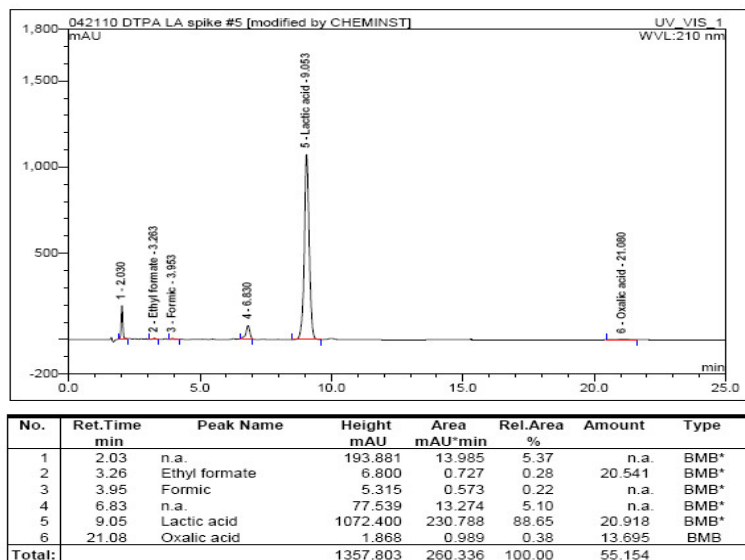


Figure 9. HPLC diode array chromatogram for 0.001 M sodium lactate at pH 3.8 irradiated to 35 kGy.

Only one degradation product for DTPA has been observed in the HPLC analysis. This product has been identified as methyliminodiacetic acid (Fig. 10). In future work, continued irradiations and methods development will ensure that a complete degradation mechanism is obtained, including examination of the effect of pH.

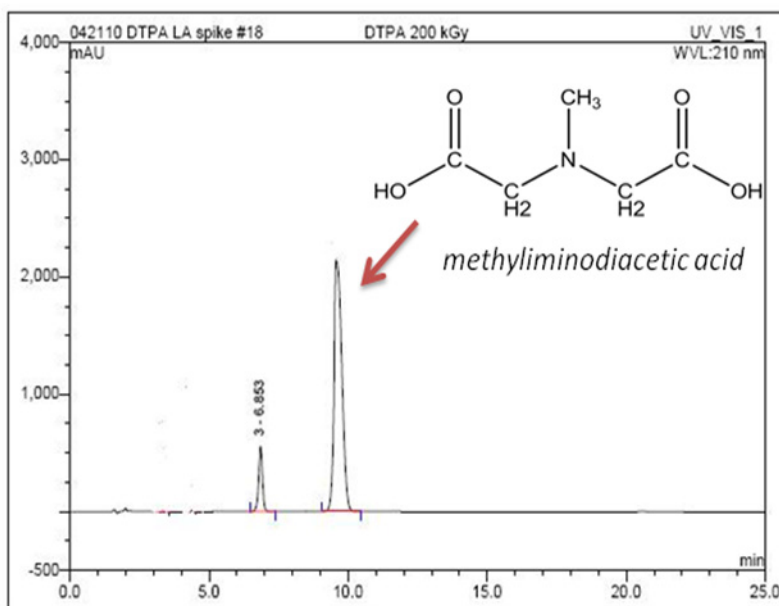


Figure 10. HPLC diode array chromatogram for 1:10 dilution DTPA irradiated to 200 kGy.

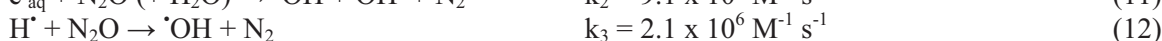
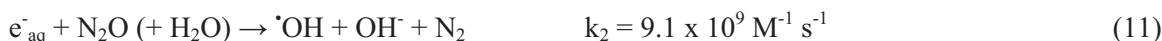
2.5 Additions to work scope

2.5.1 Metal Complexed Ligands

Previous researchers have noted that once ligands are complexed with metals, their rates of reaction with free radicals may change (Grigor'ev et al 1994). The aqueous rate constants for the reactions of •OH radical with TBP (Mincher et al 2008) and lactic acid (Martin et al 2009) have previously been reported under this program. The oxidizing •OH radical has also been found to degrade DTPA, resulting in undesirable increases in D_{Am} . Here, experiments were conducted using pulse radiolysis to measure the rate constant for •OH radical reaction with Eu-loaded DTPA. DTPA, the aqueous phase complexant used in TALSPEAK, was chosen for these initial investigations because it is readily water soluble, allowing the use of standard aqueous techniques. The •OH radical was produced by the irradiation of water which produces a mixture of radical and molecular species according to the stoichiometry:



The species in brackets are the individual G-values (yields) in $\mu\text{mol Gy}^{-1}$. By pre-saturating solutions with N_2O , conversion of the reducing hydrated electron and hydrogen atom occurs, according to the reactions:



This leads to nearly quantitative formation of oxidizing •OH radicals for kinetic investigation. The extent of •OH radical degradation is dependent upon the rate constants for the following reactions:



In this study we have determined these reaction rate constants, utilizing europium as a prototypical lanthanide. DTPA can exist in six different protonation states, dependent upon solution pH (Fig. 11). To determine rate constants for each species, •OH reaction rate constant measurements were made at several different acidic pH's. Standard thiocyanate competition kinetics was used. The change in absorbance of the $SCN_2\cdot$ radical (eq. 6) with increasing DTPA concentration is shown in Fig. 12.

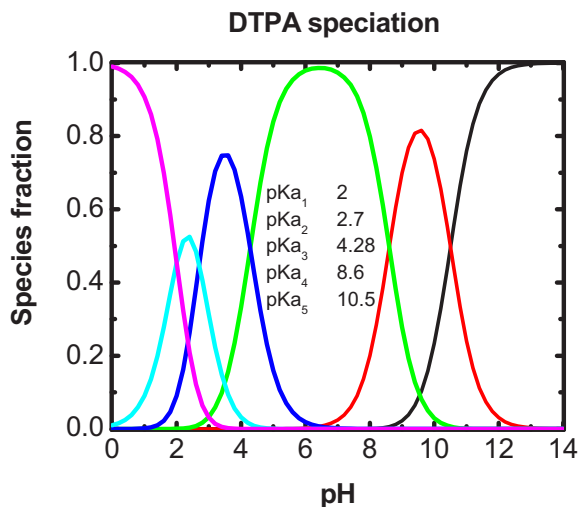


Figure 11. Occurrence of DTPA protonation species versus solution pH. Six species occur, from fully protonated to fully deprotonated.

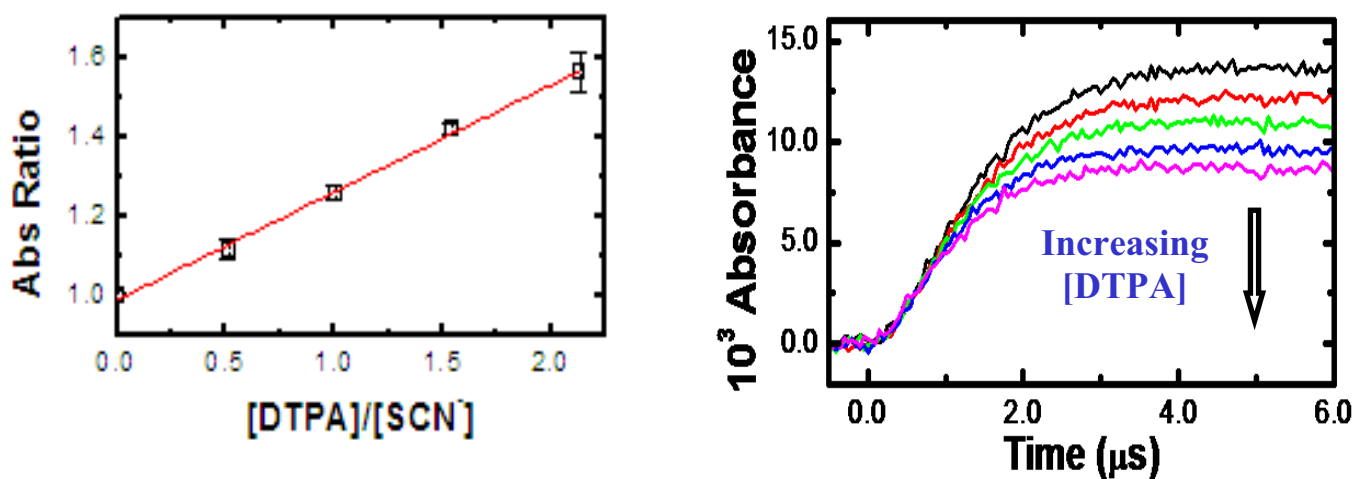


Figure 12 The linear transform plot (left) gives the bimolecular rate constant for the $\bullet OH$ radical reaction with DTPA. The decrease in SCN_2 absorbance with increasing DTPA concentration is shown on right.

Since the rate constant for eq. 6 is known, this competition between the $\bullet OH$ radical reactions can be analytically solved to give the expression:

$$\frac{Abs(SCN)_2^{\bullet-}}{Abs(SCN)_2^{\bullet-}} = 1 + \frac{k_{13}[DTPA]}{k_6[SCN^-]} \quad (15)$$

The transformation of these data gives the linear plot also shown in Fig. 12. From the fitted slope of this line, the value of the rate constant k_{13} is obtained. Rate constants determined for different pH values and the speciation of DTPA at those pHs are given in Table 2.

Table 2. Summary of speciation and measured $\bullet\text{OH}$ radical reaction rate constants for DTPA at different pHs.

pH	DTPA-H3	DTPA-H4	DTPA-H5	k ($\text{M}^{-1} \text{s}^{-1}$)
3.12	0.677	0.257	0.020	$(3.13 \pm 0.08) \times 10^9$
2.00	0.091	0.454	0.454	$(3.06 \pm 0.06) \times 10^9$
1.22	0.005	0.141	0.854	$(2.79 \pm 0.11) \times 10^9$

The resulting rate constants for the individual species, calculated based on the data of Table 2, are $3.26 \times 10^9 \text{ M}^{-1} \text{s}^{-1}$ for DTPA-H3, $3.40 \times 10^9 \text{ M}^{-1} \text{s}^{-1}$ for DTPA-H5 and $2.69 \times 10^9 \text{ M}^{-1} \text{s}^{-1}$ for DTPA-H5. It can be seen that little variation in reactivity is observed over this pH range.

In the presence of added Eu^{3+} , the $\bullet\text{OH}$ radical will react with three species, SCN^- (eq. 6), free DTPA (eq. 13) and the complexed Eu-DTPA (eq. 14). The binding constants for Eu^{3+} and DTPA are very high ($\sim 10^{20}$) and it was assumed that all the europium is fully complexed as a 1:1 complex in the presence of excess ligand. The competition equation now assumes the form shown in eq. 16, where all parameters are known other than k_{14} .

$$\frac{Abs(\text{SCN})_2^{\bullet o}}{Abs(\text{SCN})_2^{\bullet o}} = \frac{k_6[\text{SCN}^-]}{k_6[\text{SCN}^-] + k_{13}[\text{DTPA}] + k_{14}[\text{Eu} - \text{DTPA}]} \quad (16)$$

Therefore, this equation can be fitted to the decrease in absorbance of the $(\text{SCN})_2^{\bullet}$ species at 475 nm. By fitting eq. 16 to these data, the best-fit red curve (Fig. 12) is obtained. At pH 3.00, a value of $k = (5.75 \pm 0.38) \times 10^9 \text{ M}^{-1} \text{s}^{-1}$ was obtained. This rate constant is significantly higher than for the uncomplexed DTPA at this pH, which is calculated as $k_{13} = 3.08 \times 10^9 \text{ M}^{-1} \text{s}^{-1}$ from the individual values given above. When the same experiment was performed at pH 2.00, a value of $(3.86 \pm 0.06) \times 10^9 \text{ M}^{-1} \text{s}^{-1}$ was determined. This rate constant is only slightly faster than the $3.06 \times 10^9 \text{ M}^{-1} \text{s}^{-1}$ found for the uncomplexed ligand at this pH. We are presently extending these studies over a broader range of pH, and also to other metal ions such as Ce^{3+} .

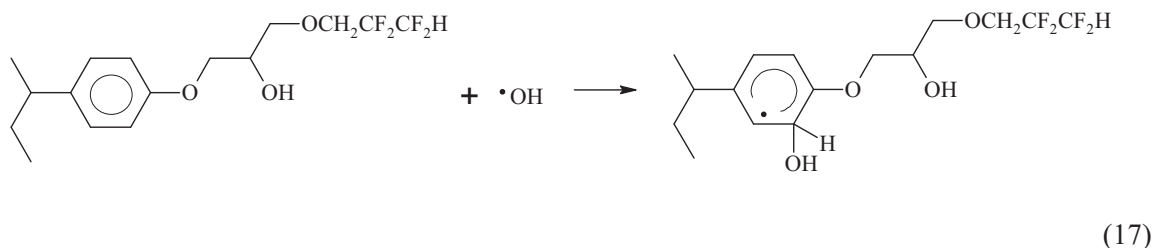
2.5.2 Cs-7SB radiation chemistry

Previously at INL, an investigation of the radiation chemistry of the FPEX process was conducted (Mincher et al 2007). This solvent extraction process was designed to partition strontium and cesium from the UREX raffinate and relied on the modifier compound Cs-7SB to ensure adequate solubility of the calixarene ligand and the calixarene and crown ether metal complexes. Despite that different ligands were used to complex cesium and strontium it was found that the loss in extraction efficiency with absorbed radiation dose was analogous for both metals. Therefore, it was concluded that radiolysis of the modifier was responsible. Subsequent to that investigation the results of a fundamental radiation chemical investigation conducted under LDRD funding (Elias et al 2010) has enabled a more insightful

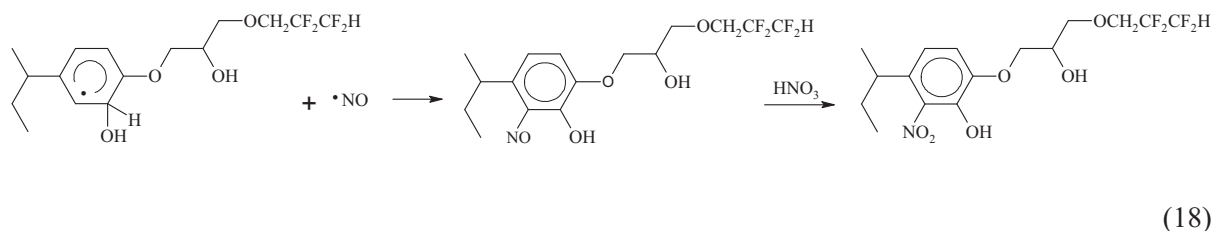
interpretation of the previous results for Cs-7SB radiolysis. Kinetic data for the free radical reactions of Cs-7SB were combined with liquid chromatography mass spectrometry results to postulate mechanisms for the oxidative nitration of Cs-7SB in irradiated nitric acid. This information was collected and used to prepare a manuscript (Swancutt et al 2010) and the discussion below is adapted from that paper.

The rate constants for the reactions of important radiolytically-produced radicals with Cs-7SB, and surrogate compounds that represent portions of the Cs-7SB molecule, are shown in Table 4. When in contact with the acidic aqueous phase, the phenyl ring of Cs-7SB is readily hydroxylated by reaction with $\cdot\text{OH}$ radical with the fast rate constant of $2.19 \times 10^9 \text{ M}^{-1} \text{ s}^{-1}$. The phenyl ring is also readily nitrated, although probably not by $\cdot\text{NO}_2$ with its low reaction rate constant of $< 10^6 \text{ M}^{-1} \text{ s}^{-1}$, or $\cdot\text{NO}_3$ radical, which has a very fast rate constant of $2.9 \times 10^9 \text{ M}^{-1} \text{ s}^{-1}$. A fast rate constant such as this suggests hydrogen abstraction rather than addition. Ring reactions, rather than side chain reactions, were confirmed by the rate constants measured for the analog compounds. Therefore, nitration probably occurs due to reaction with radiolytically-produced nitrous acid (eqs x-y). The Cs-7SB phenyl ring is activated toward this reaction by the aryl ether group, in analogy with results for anisole irradiation (Elias et al 2010). Aryl ethers should probably be avoided when designing molecules in which nitration may present problems.

Ultra Performance-Liquid Chromatography-UV- Mass Spectrometry (UPLC-UV-MS) was performed on the radiolytically-produced yellow-orange material that results from the irradiation of Cs-7SB. A major peak identified from their positive ion (AP+) mass spectra at 5.24 min retention time and two minor peaks at 5.09 and 5.17 min which were attributable to Cs-7SB and its isomers. A peak at 3.52 min corresponded to the Cs-7SB dimer. This analysis also revealed several new chromatographic peaks, including one at 3.04 min that had ions at m/z 422 and 821, which can be attributed to the sodium salt of a hydroxylated, nitrated Cs-7SB compound and its dimer. The sodium salt ions are the result of sodium hydroxide used to adjust the mobile phase pH as well as ions that may already have been present in the mobile phase components. This peak suggests hydroxyl radical-mediated nitration of Cs-7SB may be occurring. This reaction would be initiated by the kinetically fast $\cdot\text{OH}$ radical addition to the phenyl ring:



The addition reaction of the $\cdot\text{OH}$ radical results in the creation of a cyclohexadienyl radical which could then react by addition with other radicals, including the $\cdot\text{NO}$ radical, followed by oxidation:



Alternately, the hydroxylated Cs-7SB radical may stabilize by hydrogen atom addition or disproportionation, and the resulting hydroxylated Cs-7SB product may then be nitrated by the nitrous acid catalyzed nitration reaction. The nitrated, hydroxylated product was not produced in the presence of hydrazine, a nitrous acid scavenger, suggesting the importance of the nitrous acid catalyzed reaction. Additional UV spectrum peaks at 4.67 , 4.77 and 4.87 min correspond to nitrated Cs-7SB ($m/z = 387$) and its isomers. These species are probably also formed by nitrosonium ion nitration. A detailed discussion of these and other products of Cs-7SB irradiation is found in Swancutt et al (2010).

Table 3. Summary of reaction rate constants for hydroxyl radical, hydrogen atom, and nitrate radical with Cs-7SB and analogues. Reaction rates for the $\cdot\text{NO}_2$ radical were below detection limit of $\sim 10^6 \text{ M}^{-1} \text{ s}^{-1}$.

Species	$k_{\cdot\text{OH}}$ ($\text{M}^{-1} \text{ s}^{-1}$)	$k_{\text{H}\cdot}$ ($\text{M}^{-1} \text{ s}^{-1}$)	$k_{\text{NO}_3\cdot}$ ($\text{M}^{-1} \text{ s}^{-1}$)
Cs-7SB	$(2.85 \pm 0.21) \times 10^9$	$(3.17 \pm 0.11) \times 10^9$	$(2.71 \pm 0.03) \times 10^9$
methyl-2,2,3,3-tetrafluoropropyl ether	$(1.85 \pm 0.02) \times 10^8$	$(2.36 \pm 0.27) \times 10^7$	$\leq 5 \times 10^4$
4-isopropylanisole	$(1.24 \pm 0.13) \times 10^9$	$(1.04 \pm 0.05) \times 10^9$	$(2.95 \pm 0.02) \times 10^9$

2.5.3 Formic Acid/Oxalic Acid Radiolysis

In Section 1.4.3 of this report it was reported that the radiolysis of the lactic acid used in TALSPEAK results in the formation of formic and oxalic acids. However, given sufficient absorbed radiation dose the degradation of any organic compound must proceed through the formation of formic acid. Therefore we have initiated a study of formic acid radiolysis. Formic and oxalic acid solutions were prepared in 0.10 M phosphate buffer solution at different pHs: 1.30 (with HClO_4), 3.00 (with H_3PO_4), 5.01 (80:1 NaH_2PO_4 : Na_2HPO_4) and 6.75 (1:1 NaH_2PO_4 : Na_2HPO_4). Sodium formate or oxalic acid hydrate was added to each solution to give nominal 1.0 mM solutions, which were irradiated over a series of absorbed doses with ^{60}Co . Following irradiation the concentrations of formic acid, oxalic acid and glyoxalic acid were determined by HPLC.

As can be seen in Fig. 13, oxalic acid is a product of formic acid irradiation. This is probably produced by radical addition of the carboxyl radical, produced from formate hydrogen atom abstraction reactions, shown in eqs. x-y:



These reactions link the free radical chemistry of oxalic and formic acids and their respective conjugate bases. Figure 13 compares results modeled using the known rate constants for the reaction of formic acid and oxalic acid with the various radicals produced in water radiolysis with experimental results for their decomposition at pH 1.30 and 5.01 for formic acid, and at pH 3.00 and 6.75 for oxalic acid. The

agreement of the model and experimental results for the decomposition of formic and oxalic acid is good. However, for the production of oxalic acid from irradiated formic acid the model only gives about 50% of the total oxalate measured. This discrepancy implies that additional chemistry was occurring. The combined model predictions showed that glyoxylic acid was a major product in these irradiations, however, the radical-based degradation of glyoxylic acid in aqueous solution has not yet been reported. Therefore, we have also measured glyoxalic acid generation in a new series of irradiated samples. These data are currently being analyzed, and are scheduled to be presented at the Advanced Oxidation technology conference in San Diego in November, and the Pacificchem meeting in Honolulu in December.

3. CONCLUSIONS AND FUTURE WORK

The ability to measure rate constants for $\bullet\text{NO}_3$ reactions in the organic phase was an important accomplishment of the program for FY 2010. This technique will allow insights into the radiation chemistry of the organic phase which have never been previously available. These techniques will be extended to higher molecular weight alcohols to allow estimates of reaction rates in alkane solutions with limited nitrate salt solubilities. The technique proposed here for the organic phase OH radical will also be tested since this is the other important radical in irradiated solvent extraction solution.

The initiation of alpha radiolysis experiments was another major accomplishment for FY 2010. The literature contains very few references in the area of α -radiolysis effects, and some reports are contradictory. A major problem that has limited this type of research is that limited equipment is allowed for use in post-irradiation analysis of α -contaminated solutions. The development of techniques such as He-ion beam and ^{211}At irradiation to facilitate post-irradiation analyses is crucial to understanding α -radiolysis, and will support INL involvement in the recent NEUP grant issued to our collaborators. A major INL effort will be to compare α and γ -radiolysis of CMPO.

We will also continue to investigate dose rate effects, and metal complexation effects on radiation chemistry as well as continue to collect data on TALSPEAK radiation chemistry in the coming year.

4. LITERATURE CITED

- Berthon, L.; Morel, J.M.; Zorz, N.; Nicol, C.; Virelizier, H.; Madic, C. 2001, DIAMEX process for minor actinide partitioning: hydrolytic and radiolytic degradations of malonamide extractants. *Sep. Sci. Technol.* 36: 709-728.
- Buchholz, B.A.; Nuñez, L.; Vandegrift, G.F. 1996, Effect of α -radiolysis on TRUEX-NPH Solvent. *Sep. Sci. Technol.* 31: 2231-2243.
- Camès, B; Bisel, I.; Baron, P.; Rudloff, D.; Saucerotte, B. 2010, DIAMEX solvent behavior under continuous degradation and regeneration operations, In: Nuclear Energy and the Environment, ACS Symposium Series 1046, Wai, C.M.; Mincher, B.J., Eds. American Chemical Society, Washington DC, USA.
- Ekberg, C.; Aneheim, E.; Fermvik, A.; Skarnemark, G. 2010, Using ^{211}At as an internal alpha radiolysis source allowing simple detection of radiolysis products. *Radiat. Phys. Chem.* 79:454-456.
- Elias, G.; Mincher, B.J.; Mezyk, S.P.; Cullen, T.; Martin, L.R. 2010, Anisole nitration during gamma-irradiation of aqueous nitrite and nitrate solutions. Free radical versus ionic mechanisms. *Environ. Chem.* 7:183-187.
- Fermvik, A.; Ekberg, C.; Englund, S.; Foreman, M.R.St.J.; Modolo, G.; Retegan, T.; Skarnemark, G. 2009, Influence of dose rate on the radiolytic stability of a BTBP solvent for actinide(III)/lanthanide(III) separation. *Radiochim. Acta* 97:319-324.
- Grigor'ev, E.I.; Mikhailitsyna, O.V.; Nesterov, S.V.; Trakhtenberg, L.I. 1994, Radiation stability of 15-crown-5 complexes with alkaline earth metal chlorides. *Mendeleev Commun.* 4:66-67.
- Groenewold, G.S.; Appelhans, A.D.; McIlwain, M.E.; Gresham, G.L. 2010, Characterization of coordination complexes by desorption electrospray mass spectrometry with a capillary target, *Int. J. of Mass Spectrom.*, in press.
- Magnusson, D.; Christiansen, B.; Malmbeck, R.; Glatz, J.-P. 2009, Investigation of radiolytic stability of a CyMe4-BTBP based SANEX solvent. *Radiochim. Acta* 97:497-502.
- Martin, L.R.; Mezyk, S.P.; Mincher, B.J. 2009, Determination of Arrhenius and thermodynamic parameters for the aqueous reaction of the hydroxyl radical with formic acid. *J. Phys. Chem. A* 113:141-145.
- Mezyk, S.P.; Nilsson, M.; Mincher, B.J. 2010, NEUP 10-910: Alpha Radiolysis of Nuclear Solvent Extraction Ligands used for An(III) and Ln(III) Separations (FCS-3).
- Mincher, B.J. 2010, Irradiation affects on neptunium oxidation states. Proceedings of Acsept 2010, Bologna, Italy.
- Mincher, B.J.; Mezyk, S.P.; Martin, L.R. 2008, A pulse radiolysis investigation of the reactions of tributylphosphate with the radical products of aqueous nitric acid irradiation. *J. Phys. Chem.* 112:6275-6280.

- Mincher, B.J.; Mezyk, S.P.; Bauer, W.F.; Elias, G.; Riddle, C.; Peterman, D.R. 2007, FPEX γ -radiolysis in the presence of nitric acid. *Solvent Extr. Ion Exch.* 25:593-601.
- Mitroka, S.; Zimmeck, S.; Troya, D.; Tanko, J.M. 2010, How solvent modulates hydroxyl radical reactivity in hydrogen atom abstractions. *J. Am. Chem. Soc.* 132:2907-2913.
- Nilsson, M.; Nash, K.L. 2007, Review article: A review of the development and operational characteristics of the TALSPEAK process. *Solvent Extr. Ion Exch.* 25:665-701.
- Pastina, B.; LaVerne, J.A. 1999, Hydrogen peroxide production in the radiolysis of water with heavy ions. *J. Phys. Chem. A* 103, 1592-1597.
- Sugo, Y.; Taguchi, M.; Sasaki, Y.; Hirota, K.; Kimura, T. 2009, Radiolysis study of actinide complexing agent by irradiation with helium ion beam. *Radiat. Phys. Chem.* 78:1140-1144.
- Swancutt, K.L.; Cullen, T.D.; Mezyk, S.P.; Elias, G.; Bauer, W.L.; Peterman, D.R.; Riddle, C.L.; Ball, R.D.; Mincher, B.J.; Muller, J.J. 2010, The radiation chemistry of the Cs-7SB modifier used in Cs and Sr solvent extraction. *Solvent Extr. Ion Exch.*, in review.
- Tachimori S. 1979, Radiation effects on the extraction of americium(III) with di(2-ethylhexyl) phosphoric acid. *J. Radioanal. Chem.* 50:133-142.
- Tachimori, S. 1979b Synergistic extraction of americium with MEHPA-DEHPA mixed solvent from nitric acid solution. *J. Radioanal. Chem.* 49:31-35.
- Tahraoui, A.; Morris, J.H. 1995, Decomposition of solvent extraction media during nuclear reprocessing: literature review. *Sep. Sci. Technol.* 30: 2603-2630.